Volume 23
Number 7
21 February 2021
Pages 1531–1686

CrystEngComm

rsc.li/crystengcomm

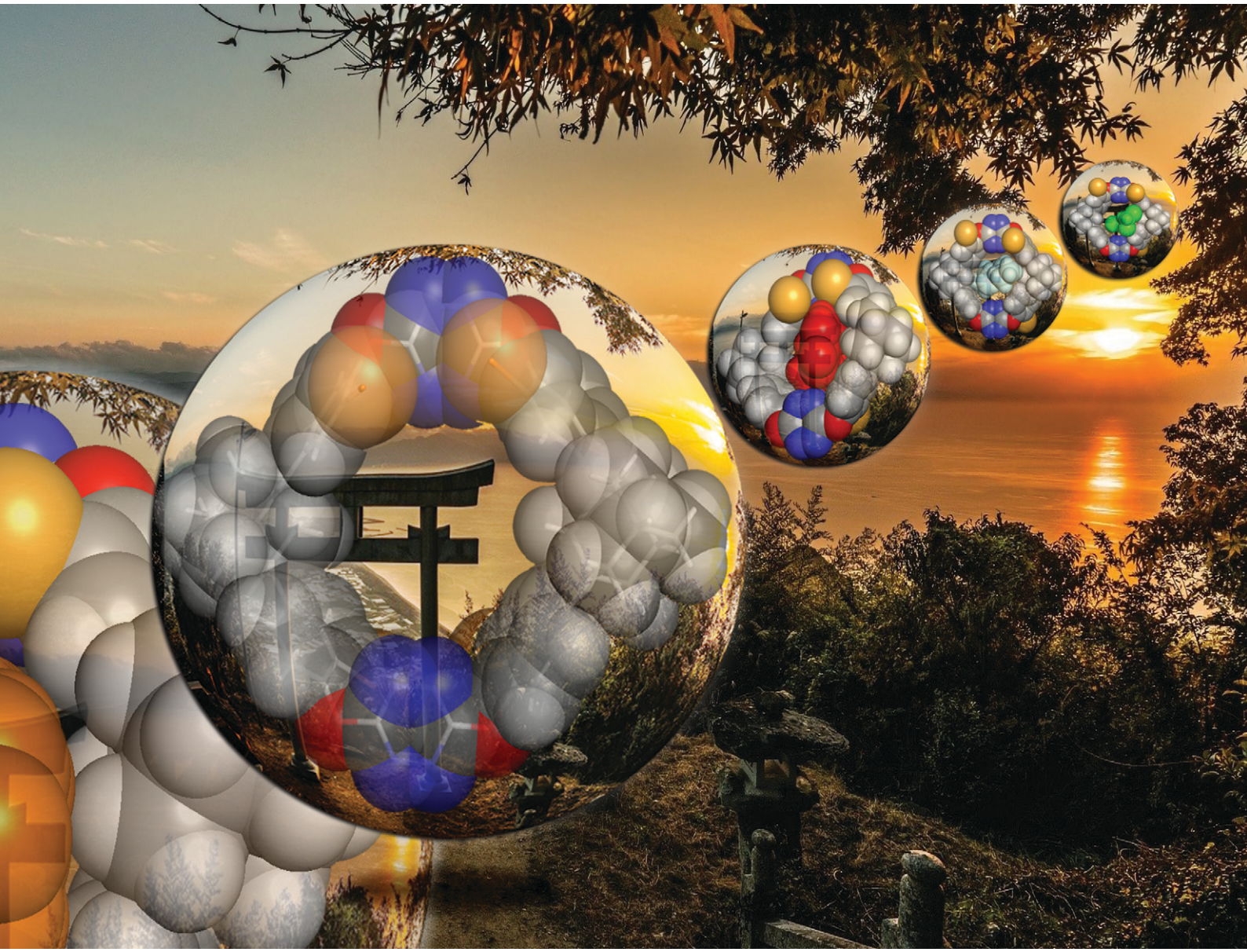

ISSN 1466-8033

ROYAL SOCIETY OF CHEMISTRY

COMMUNICATION

Masahide Tominaga, Kentaro Yamaguchi *et al.*
Guest-dependent single-crystal-to-single-crystal transformations in porous adamantane-bearing macrocycles

ROYAL SOCIETY OF CHEMISTRY

Royal Society of Chemistry approved training courses

Explore your options.
Develop your skills.
Discover learning that suits you.

Courses in the classroom, the lab, or online

Find something for every stage of your professional development. Search our database by:

- subject area
- location
- event type
- skill level

Members **get at least 10% off**

Visit **rsc.li/cpd-training**

SAVE 10%

CrystEngComm

ROYAL SOCIETY OF CHEMISTRY

COMMUNICATION

Cite this: *CrystEngComm*, 2021, **23**, 1539

Received 9th December 2020,
Accepted 11th January 2021

DOI: 10.1039/d0ce01782e

rsc.li/crystengcomm

Guest-dependent single-crystal-to-single-crystal transformations in porous adamantane-bearing macrocycles†

Tadashi Hyodo, Masahide Tominaga * and Kentaro Yamaguchi *

An adamantane-bearing macrocycle showed permanent intrinsic porosity and adsorption of small organic compounds in a single-crystal-to-single-crystal fashion. Guest uptake by the porous crystals gave rise to the structural transformation of the supramolecular organic framework, resulting in the change of shape and size of one-dimensional pores.

Porous materials have attracted prominent attention in a wide variety of fields due to their potential and practical applications in gas storage and separation, heterogeneous catalysis, and chemical sensing.[1–5] Zeolites, metal–organic frameworks (MOFs), and covalent organic frameworks (COFs) are representative porous solids that are effectively constructed by diverse methodologies and approaches.[6–10] The porosity of macrocycles, including calixarenes, cucurbiturils, and pillararenes, was energetically explored because the solubility of these macrocycles in common organic solvents and their mild reaction conditions provide fascinating advantages in processability, in contrast to insoluble porous frameworks and networks.[11–14] The frameworks built from macrocyclic compounds are generally less stable than those from other porous materials because of the constructions by weak intermolecular interactions. Therefore, macrocycle-based crystals possessing intrinsic and extrinsic pores tend to collapse after solvent removal by heating. Shimizu and co-workers reported that a series of macrocyclic bis-urea molecules were formed into hydrogen-bonded crystalline materials made up of tubular structures containing one-dimensional (1D) channels, which exhibited permanent porosity and inclusion of various small organic compounds.[15,16] The porous crystals of macrocyclic imines were exploited by Costa's group and applied to the crystalline sponge method.[17,18] Hisaki and co-workers disclosed that a C_3-symmetric macrocycle possessing carboxyl groups is a powerful building block to access a multiporous, hydrogen-bonded, hexagonal network that exhibits CO_2 gas adsorption.[19,20]

Single-crystal-to-single-crystal (SCSC) transformations, such as guest exchange and phase transition in porous solids, are an important phenomenon from which the precise structural information of adsorptive guests and supramolecular organic frameworks is obtained by single-crystal X-ray diffraction methods.[21–23] In addition, the quantitative assessment of dominant intermolecular interactions between individual components is possible by Hirshfeld surface analysis.[24,25] In contrast to MOFs, there are few studies on dynamic behaviors triggered by external stimuli in porous solids of macrocycles.[26–28] In this context, we report herein the preparation of permanently porous crystals composed of network structures possessing tubular architectures from a bromine-substituted adamantane-based macrocycle (**1**). The dynamic behaviors of the frameworks accompanied by the conformational changes of **1** were showed through the adsorption and desorption of guests, leading to the alteration of the shape and size of 1D pores. Meanwhile, the incorporation of other guests into the porous crystals maintained their frameworks. These processes occurred in the SCSC fashion and were monitored by X-ray analysis.

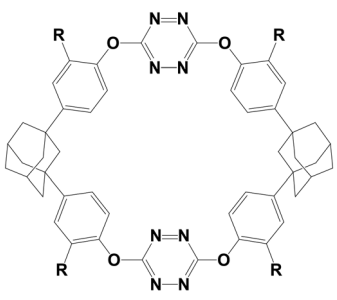

Fig. 1 Adamantane-bearing macrocycles with tetrazine units (**1**, **2**).

Faculty of Pharmaceutical Sciences at Kagawa Campus, Tokushima Bunri University, 1314-1 Shido, Sanuki, Kagawa 769-2193, Japan.
E-mail: tominagam@kph.bunri-u.ac.jp, kyamaguchi@kph.bunri-u.ac.jp

† Electronic supplementary information (ESI) available: NMR spectra, Hirshfeld surfaces, 2D fingerprint plots, and crystallographic information files (CIFs) of crystals **1b**–**1e**. CCDC 2014531–2014534. For ESI and crystallographic data in CIF or other electronic format see DOI: 10.1039/d0ce01782e

Recently, we described that the nucleophilic aromatic substitution reactions of disubstituted adamantanes possessing halophenol units and 3,6-dichlorotetrazine afforded macrocycles (**1**, **2**) and their [2]catenanes (Fig. 1).[29] In the crystalline state, both macrocycles had a hexagonal structure with a cavity, and were formed into network structures consisted of tubular architectures. Empty crystal **2a** without solvents, which was prepared from macrocycle **2**, exhibited permanent porosity and inclusion of green leaf volatiles in the SCSC fashion, and the liquid guests were identified by X-ray analysis. The applicability of porous macrocycle-based organic crystals to the crystalline sponge method could be attributed to the robustness of the supramolecular organic frameworks of macrocycle **2**, which is derived from the van der Waals forces and the halogen bonding interactions. On the other hand, the porosity of crystal **1** has not been examined yet.

The guest exchange of crystal **1a** containing dichloromethane as the crystallization solvent was carried out by the immersion of the crystal in diethyl ether (Fig. S1 in the ESI†). From the X-ray analysis of the resulting crystal (**1b**), the conformation and packing of **1** were similar to those of the initial crystals (Fig. 2a). The macrocycle in crystal **1b** had a hexagonal structure with a cavity. The centroid-to-centroid distances between the aromatic or aliphatic units were 11.71 Å for the tetrazine rings, 10.88 and 11.21 Å for the two pairs of benzene rings, and 13.63 Å for the adamantane units. The two pairs of two bromine atoms were positioned at the top and bottom rims with respect to the macrocyclic planes consisted of the linking oxygen atoms and located on or laterally towards the macrocyclic skeleton. Diethyl ethers were accommodated within the cavity of **1**. The macrocycles were fabricated to give a molecular network composed of tubular structures through CH···Br interactions between the hydrogen atom of the adamantane parts and the bromine atoms and halogen···π interactions between the bromobenzene parts (Fig. 3a).[30,31]

The treatment of crystal **1b** under vacuum for 24 h at 100 °C gave crystal **1c** with empty channels. The crystal size and morphology were almost intact. The ^{1}H NMR spectrum of crystal **1c** dissolved in $CDCl_3$ also confirmed the absence of the

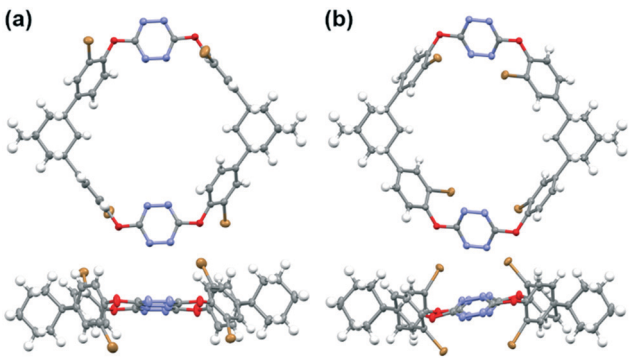

Fig. 2 Top and side views of the molecular structures of **1** in crystals (a) **1b** and (b) **1c**. Solvent molecules are omitted for clarity.

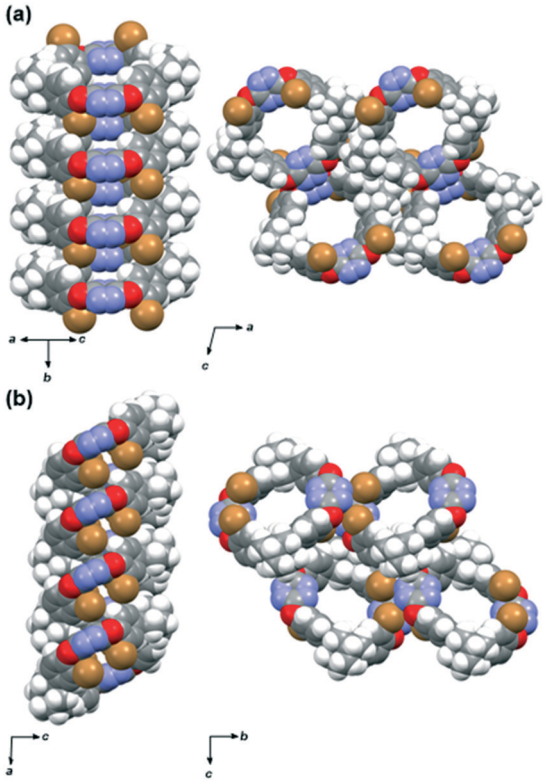

Fig. 3 Packing diagrams of **1** in side views of the tubular structures and top views of the network structures in crystals (a) **1b** and (b) **1c**. Solvent molecules are omitted for clarity.

used solvent within the crystal. Remarkably, the conformation and arrangement of **1** in crystal **1c** were considerably different from those of **1** in crystal **1b** (Fig. 2b). The macrocycle had a slightly distorted hexagonal structure as shown in crystal **1c**. The centroid-to-centroid distance between the tetrazine rings was longer, whereas that between the adamantane parts was shorter than those in crystal **1b**. All the bromine atoms internally faced the macrocyclic skeleton, and the tetrazine rings were tilted obliquely towards the macrocyclic planes. The macrocycles were aligned to form tubular structures *via* CH···Br interactions between the hydrogen and bromine atoms of the bromobenzene parts and CH···π interactions between the hydrogen atoms of the adamantane units and the bromobenzene parts, and these tubular structures were assembled into network structures *via* Br···N interactions between the bromine and nitrogen atoms and CH···O interactions between the hydrogen atoms of the adamantane parts and the oxygen atoms (Fig. 3b). Compared with crystal **1b**, the pore shape in crystal **1c** changed from hexagonal to nearly rectangular, and the macrocycles were tilted from the vertical position along the 1D pores.

To evaluate the robustness of porous crystal **1c**, relative quantification between macrocycles was performed using Hirshfeld surface analysis and related 2D fingerprint plots (Fig. S2 in the ESI†).[24,25] Multiple intermolecular interactions between macrocycles, the main ones being H···H contacts (31.9%), Br···H contacts (9.2%), and N···H contacts (8.9%),

contribute to the preservation of the crystalline lattices. The variation of bromine atoms between crystals **1b** and **1c** was outstanding. The distances between the bromine atoms and the hydrogen atoms of the bromobenzene parts or the center of the tetrazine rings of adjacent macrocycles in the tubular assemblies were 5.83 Å and 5.96 Å for crystal **1b** and 2.99 Å and 4.05 Å for crystal **1c** (Fig. 4 and S5 and S7 in the ESI†). As a result of the desorption of diethyl ether, the macrocycles were inclined from the vertical position along the channel axis in response to the reduction of the distances between the bromine atoms and the hydrogen atoms of the bromobenzene parts or the tetrazine rings involving in the halogen-related interactions. Subsequently, the structural change of the tubular assemblies culminated in different structures of the entire molecular networks. The calculated pore volume of the unit cell was 24.1% for crystal **1b** and 16.5% for crystal **1c** (Fig. S3 in the ESI†). In crystal **1c**, recessed regions were observed in the 1D channels.

Crystal **1c** returned to its original crystal structure containing diethyl ether after soaking in diethyl ether for 24 h at room temperature. The conformation and frameworks of **1** in the resulting crystal were nearly identical to those of crystal **1b**. The conformations of the included guests and their orientation in **1** were also similar to those in **1b**. From these experimental outcomes, we concluded that the porous crystals of adamantane-based macrocycles could be reversibly and mutually converted to two different molecular networks through the adsorption and desorption of diethyl ether (Fig. 6).

To examine the uptake of other guests, we selected two aromatic compounds: styrene (**3**) and ethylbenzene (**4**). Compound **3** is one of the most well-known aromatic compounds in the petrochemical industry, and is employed as a raw material for the polymerization into synthetic rubbers and resins.[32] The dehydrogenation of **4** produced a mixture of **4** and **3**. These two aromatic compounds have similar boiling points and molecular shapes, and are therefore difficult to separate. Diverse zeolites and MOFs have been developed as absorbents to separate the two compounds.[33,34] Previously, Huang and Cooper demonstrated that pillar[6]arene is an excellent absorbent as a nonporous macrocycle-based material for the separation of **3** over **4**.[35] The uptake of **3** and **4** by porous crystal was tested. The immersion of crystal **1c** in **3** or **4** for 24 h provided clathrate crystals (**1d**, **1e**). The conformations and arrangements of **1** were unchanged, in contrast to when diethyl ether was used (Fig. 6). The guest molecules were disordered in both crystals, and one conformer of **3** or **4** per asymmetric unit appeared. **3** was accommodated within the cavities through CH···N interactions between the hydrogen atoms of the vinyl groups and the benzene rings of **3** and the nitrogen atoms of the tetrazine rings (Fig. 5a). **4** was also captured within the cavities *via* CH···N interactions between the hydrogen atoms of the benzene rings of **4** and the nitrogen atoms of the tetrazine rings (Fig. 5b). The stoichiometric ratio of **1** and the

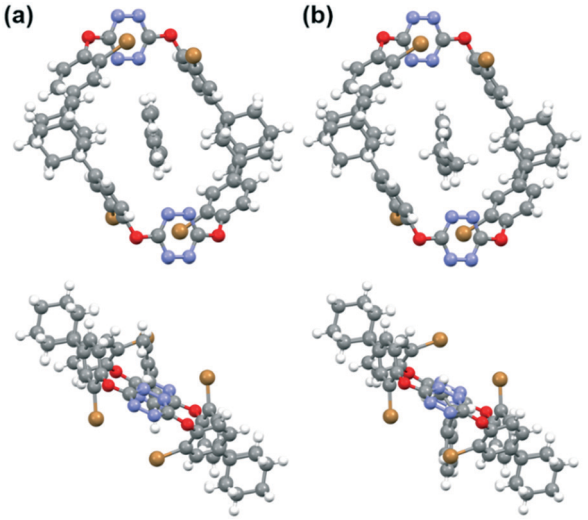

Fig. 5 Top and side views of the molecular structures of **1** and the guests in crystals (a) **1d** and (b) **1e**. Disordered atoms are omitted for clarity.

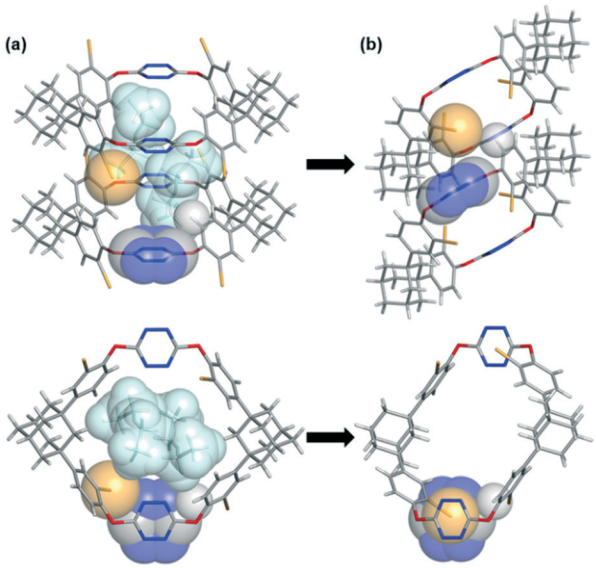

Fig. 4 Shrinkage and inclination of the macrocycles in the tubular structures of the porous crystals culminated in the desorption of diethyl ether. Side and top views of the molecular packing of **1** in crystals (a) **1b** and (b) **1c**. Diethyl ether is colored light blue for clarity.

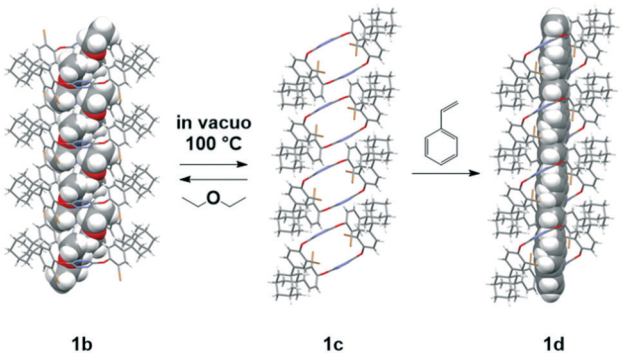

Fig. 6 Schematic representation of the dynamic behaviors in the porous crystals of the adamantane-bearing macrocycle.

guest was approximately 1 : 1 for both crystals, based on crystal structure determination and ^{1}H NMR analysis of a solution of the crystals in $CDCl_3$ (Fig. S4 in the ESI†). Both aromatic guests were located along the channel axis, and the benzene rings of **3** were sandwiched by the two tetrazine rings unlike those of **4**. Moreover, the vinyl group of **3** was positioned in the plane of the benzene ring, whereas **4** was non-planar. From these results, the orientations of the two aromatic guests in the macrocycle were different. Among various porous organic crystals of macrocycles,[36–39] the uptake of vaporized aromatic compounds was mostly treated in the solid–gas phase. It is noteworthy that the porous crystals of adamantane-bearing macrocycle could capture **3** and **4** in the solid–liquid phase.

The capture by empty crystal **2a** was attempted and compared with that by crystal **1c** in conjunction to the difference in pore size and shape. When crystal **2a** was immersed in **3** or **4**, the crystal gradually and partly dissolved. Crystal **1c** was less soluble in **3** or **4**, indicating that the framework of **1** is more robust than that of **2** for the two aromatic compounds in the crystalline state. This is perhaps attributable to the smaller pore volume of empty crystal **1c** than that of crystal **2a**. The calculated void volumes of crystals **1c** and **2a** are 401.0 Å^3 and 630.0 Å^3. Moreover, as regards the strength of halogen-related interactions, the bromine atoms on the macrocycles showed a stronger interaction than the chlorine atoms.

In summary, we demonstrated that the porous crystals of adamantane-bearing macrocycles exhibited uptake of guest molecules and structural transformation in the SCSC fashion. Guest exchange of crystal **1a** possessing dichloromethane afforded crystal **1b** containing diethyl ether, and **1b** was transformed into empty crystal **1c** having a structurally different form through thermal treatment under vacuum. The supramolecular organic frameworks in crystal **1c** were restored into the same as those in crystal **1b** by the adsorption of diethyl ether. Furthermore, the inclusion of styrene and ethylbenzene by crystal **1c** was realized, where the conformation and arrangement of **1** were preserved. Halogen interactions participated in these dynamic SCSC transformations. Porous crystals of adamantane-based macrocycles are convenient and intriguing host materials for the adsorption and structural determination of liquid organic compounds.

This work was partly supported by JSPS KAKENHI Grant Numbers JP19K05591 and JP19K05447.

Conflicts of interest

There are no conflicts of interest to declare.

Notes and references

1 M. O'Keeffe and O. M. Yaghi, *Chem. Rev.*, 2012, **112**, 675–702.
2 A. Karmakar, P. Samanta, A. V. Desai and S. K. Ghosh, *Acc. Chem. Res.*, 2017, **50**, 2457–2469.
3 A. I. Cooper, *ACS Cent. Sci.*, 2017, **3**, 544–553.
4 M. Mastalerz, *Acc. Chem. Res.*, 2018, **51**, 2411–2422.
5 X. Chen, K. Geng, R. Liu, K. T. Tan, Y. Gong, Z. Li, S. Tao, Q. Jiang and D. Jiang, *Angew. Chem., Int. Ed.*, 2020, **59**, 5050–5091.
6 G. Distefano, H. Suzuki, M. Tsujimoto, S. Isoda, S. Bracco, A. Comotti, P. Sozzani, T. Uemura and S. Kitagawa, *Nat. Chem.*, 2013, **5**, 335–341.
7 T. Drake, P. Ji and W. Lin, *Acc. Chem. Res.*, 2018, **51**, 2129–2138.
8 E. Jin, M. Asada, Q. Xu, S. Dalapati, M. A. Addicoat, M. A. Brady, H. Xu, T. Nakamura, T. Heine, Q. Chen and D. Jiang, *Science*, 2017, **357**, 673–676.
9 W. Ji, L. Xiao, Y. Ling, C. Ching, M. Matsumoto, R. P. Bisbey, D. E. Helbling and W. R. Dichtel, *J. Am. Chem. Soc.*, 2018, **140**, 12677–12681.
10 H. L. Nguyen, N. Hanikel, S. J. Lyle, C. Zhu, D. M. Proserpio and O. M. Yaghi, *J. Am. Chem. Soc.*, 2020, **142**, 2218–2221.
11 H. Kim, Y. Kim, M. Yoon, S. Lim, S. M. Park, G. Seo and K. Kim, *J. Am. Chem. Soc.*, 2010, **132**, 12200–12202.
12 R. S. Patil, D. Banerjee, C. Zhang, P. K. Thallapally and J. L. Atwood, *Angew. Chem., Int. Ed.*, 2016, **55**, 4523–4526.
13 K. Jie, Y. Zhou, E. Li and F. Huang, *Acc. Chem. Res.*, 2018, **51**, 2064–2072.
14 T. Ogoshi, T. Kakuta and T. Yamagishi, *Angew. Chem., Int. Ed.*, 2019, **58**, 2197–2206.
15 L. S. Shimizu, S. R. Salpage and A. A. Korous, *Acc. Chem. Res.*, 2014, **47**, 2116–2127.
16 A. J. Sindt, M. D. Smith, S. Berens, S. Vasenkov, C. R. Bowers and L. S. Shimizu, *Chem. Commun.*, 2019, **55**, 5619–5622.
17 E. Sanna, E. C. Escudero-Adán, A. Bauzá, P. Ballester, A. Frontera, C. Rotger and A. Costa, *Chem. Sci.*, 2015, **6**, 5466–5472.
18 E. Sanna, E. C. Escudero-Adán, C. López, P. Ballester, C. Rotger and A. Costa, *J. Org. Chem.*, 2016, **81**, 5173–5180.
19 I. Hisaki, S. Nakagawa, N. Tohnai and M. Miyata, *Angew. Chem., Int. Ed.*, 2015, **54**, 3008–3012.
20 I. Hisaki, S. Nakagawa, N. Ikenaka, Y. Imamura, M. Katouda, M. Tashiro, H. Tsuchida, T. Ogoshi, H. Sato, N. Tohnai and M. Miyata, *J. Am. Chem. Soc.*, 2016, **138**, 6617–6628.
21 K. Biradha, Y. Hongo and M. Fujita, *Angew. Chem., Int. Ed.*, 2002, **41**, 3395–3398.
22 Y. Sakata, S. Furukawa, M. Kondo, K. Hirai, N. Horike, Y. Takashima, H. Uehara, N. Louvain, M. Meilikhov, T. Tsuruoka, S. Isoda, W. Kosaka, O. Sakata and S. Kitagawa, *Science*, 2013, **339**, 193–196.
23 K. Rissanen, *Chem. Soc. Rev.*, 2017, **46**, 2638–2648.
24 M. A. Spackman and D. Jayatilaka, *CrystEngComm*, 2009, **11**, 19–32.
25 M. J. Turner, J. J. McKinnon, S. K. Wolff, D. J. Grimwood, P. R. Spackman, D. Jayatilaka and M. A. Spackman, *CrystalExplorer17*, University of Western Australia, 2017.
26 S. J. Dalgarno, P. K. Thallapally, L. J. Barbour and J. L. Atwood, *Chem. Soc. Rev.*, 2007, **36**, 236–245.
27 Y. Wang, K. Xu, B. Li, L. Cui, J. Li, X. Jia, H. Zhao, J. Fang and C. Li, *Angew. Chem., Int. Ed.*, 2019, **58**, 10281–10284.

28 Y. Zhou, K. Jie, R. Zhao and F. Huang, *J. Am. Chem. Soc.*, 2019, **141**, 11847–11851.
29 M. Tominaga, T. Hyodo, Y. Maekawa, M. Kawahata and K. Yamaguchi, *Chem. – Eur. J.*, 2020, **26**, 5157–5161.
30 A. Mukherjee, S. Tothadi and G. R. Desiraju, *Acc. Chem. Res.*, 2014, **47**, 2514–2524.
31 G. Cavallo, P. Metrangolo, R. Milani, T. Pilati, A. Priimagi, G. Resnati and G. Terraneo, *Chem. Rev.*, 2016, **116**, 2478–2601.
32 K. Othmer, *Encyclopedia of Chemical Technology*, John Wiley and Sons Inc., 2008, p. 1040.
33 M. Maes, F. Vermoortele, L. Alaerts, S. Couck, C. E. A. Kirschhock, J. F. M. Denayer and D. E. De Vos, *J. Am. Chem. Soc.*, 2010, **132**, 15277–15285.
34 S. Mukherjee, B. Joarder, A. V. Desai, B. Manna, R. Krishna and S. K. Ghosh, *Inorg. Chem.*, 2015, **54**, 4403–4408.
35 K. Jie, M. Liu, Y. Zhou, M. A. Little, S. Bonakala, S. Y. Chong, A. Stephenson, L. Chen, F. Huang and A. I. Cooper, *J. Am. Chem. Soc.*, 2017, **139**, 2908–2911.
36 M. Wang, J. Zhou, E. Li, Y. Zhou, Q. Li and F. Huang, *J. Am. Chem. Soc.*, 2019, **141**, 17102–17106.
37 X. Sheng, E. Li, Y. Zhou, R. Zhao, W. Zhu and F. Huang, *J. Am. Chem. Soc.*, 2020, **142**, 6360–6364.
38 Y. Zhou, K. Jie, R. Zhao, E. Li and F. Huang, *J. Am. Chem. Soc.*, 2020, **142**, 6957–6961.
39 Y. Wu, J. Zhou, E. Li, M. Wang, K. Jie, H. Zhu and F. Huang, *J. Am. Chem. Soc.*, 2020, **142**, 19722–19730.